Research Article

Cancer Immunology Research

Dual PD-1 and CTLA-4 Checkpoint Blockade Promotes Antitumor Immune Responses through CD4$^+$Foxp3$^-$ Cell–Mediated Modulation of CD103$^+$ Dendritic Cells

Paul A. Beavis[1,2], Melissa A. Henderson[1,2], Lauren Giuffrida[1,2], Alexander J. Davenport[1,2], Emma V. Petley[1,2], Imran G. House[1,2], Junyun Lai[1,2], Kevin Sek[1,2], Nicole Milenkovski[1,2], Liza B. John[1,2], Sherly Mardiana[1,2], Clare Y. Slaney[1,2], Joseph A. Trapani[1,2], Sherene Loi[1,2], Michael H. Kershaw[1,2,3], Nicole M. Haynes[1,2], and Phillip K. Darcy[1,2,3,4]

Abstract

Immunotherapy is widely accepted as a powerful new treatment modality for the treatment of cancer. The most successful form of immunotherapy to date has been the blockade of the immune checkpoints PD-1 and CTLA-4. Combining inhibitors of both PD-1 and CTLA-4 increases the proportion of patients who respond to immunotherapy. However, most patients still do not respond to checkpoint inhibitors, and prognostic biomarkers are currently lacking. Therefore, a better understanding of the mechanism by which these checkpoint inhibitors enhance antitumor immune responses is required to more accurately predict which patients are likely to respond and further enhance this treatment modality. Our current study of two mouse tumor models revealed that CD4$^+$Foxp3$^-$ cells activated by dual PD-1/CTLA-4 blockade modulated the myeloid compartment, including activation of conventional CD103$^+$ dendritic cells (DC) and expansion of a myeloid subset that produces TNFα and iNOS (TIP-DCs). CD4$^+$Foxp3$^-$ T cell–mediated activation of CD103$^+$ DCs resulted in enhanced IL12 production by these cells and IL12 enhanced the therapeutic effect of dual PD-1/CTLA-4 blockade. Given the importance of these myeloid subsets in the antitumor immune response, our data point to a previously underappreciated role of CD4$^+$Foxp3$^-$ cells in modulating this arm of the antitumor immune response. *Cancer Immunol Res; 6(9); 1069–81. ©2018 AACR.*

Introduction

The immune system plays a vital role in the control of malignant neoplasms, and infiltration of tumors with immune cells correlates with favorable prognosis in several cancer types (1–3). Immunotherapy is now a major treatment modality in cancer (4–8), particularly the use of checkpoint inhibitors, which block the interactions used by the tumor to suppress effector T-cell function (9). The combination of anti–CTLA-4 and inhibitors of the PD-1: PDL-1/PDL-2 interaction is highly efficacious (6, 8, 10, 11), but the mechanism by which this synergy occurs remains relatively unknown, and predictive prognostic markers are lacking (12). These checkpoint inhibitors work in distinct ways (6, 13): PD-1 blockade is thought to predominantly enhance the function of CD8$^+$ T cells within the tumor where the CD8$^+$ T cells encounter high-expressing PDL-1$^+$ tumor cells and PDL-1$^+$/PDL-2$^+$ stromal cells (14–16). Although CTLA-4 is also expressed on intratumoral CD8$^+$ T cells and potentially limits their activity through interaction with CD80/CD86 at the tumor site (17), anti–CTLA-4 also offers therapeutic benefit through the priming of antitumor T-cell responses in the draining lymph nodes (DLN). The therapeutic efficacy of anti–CTLA-4 may also be partly attributed to the depletion of CD4$^+$Foxp3$^+$ cells, due to their constitutively high expression of CTLA-4 (18, 19). These distinct mechanisms of action for anti–PD-1 and anti–CTLA-4 may partially explain the increased efficacy observed following combination therapy.

Although CD4$^+$ T cells can recognize neoantigens expressed by cancers (20–23) and it has been reported that anti–PD-1/anti–CTLA-4 combination therapy activates CD4$^+$Foxp3$^-$ cells (24, 25), little is known of the mechanism and consequence of this activation. In the current study, we investigated whether the combination of anti–PD-1/anti–CTLA-4 therapy could activate CD4$^+$Foxp3$^-$ cells and explored the mechanism underpinning the increase in antitumor efficacy. We observed that combination therapy significantly activated CD4$^+$Foxp3$^-$ effector cells resulting in the activation of tumor-infiltrating CD103$^+$ DCs, a cell important for tumor-antigen presentation and efficacy of checkpoint inhibitors (26–30). Activation of CD4$^+$Foxp3$^-$ cells was sufficient to stimulate CD103$^+$ DCs, shown by the increased IL12 production by these cells in mice depleted of both CD8$^+$ T cells and CD4$^+$Foxp3$^+$ cells. The activation of CD4$^+$ T cells was partially

[1]Cancer Immunology Program, Peter MacCallum Cancer Centre, Melbourne, Victoria, Australia. [2]Sir Peter MacCallum Department of Oncology, The University of Melbourne, Parkville, Melbourne, Victoria, Australia. [3]Department of Pathology, University of Melbourne, Parkville, Melbourne, Victoria, Australia. [4]Department of Immunology, Monash University, Clayton, Melbourne, Victoria, Australia.

Note: Supplementary data for this article are available at Cancer Immunology Research Online (http://cancerimmunolres.aacrjournals.org/).

Corresponding Authors: Phillip K. Darcy, Cancer Immunology Program, Peter MacCallum Cancer Center, Victoria, Australia. Phone: 613-8559-7093; E-mail: phil.darcy@petermac.org; and Paul A. Beavis, Phone: 613-8559-5051; E-mail: paul.beavis@petermac.org

doi: 10.1158/2326-6066.CIR-18-0291

dependent on IL12, indicating a previously undescribed link between tumor-infiltrating CD103$^+$ DCs and T_H1 like CD4$^+$Foxp3$^-$ cells in the context of checkpoint inhibition. These results indicate that dual PD-1/CTLA-4 blockade can robustly activate a CD4$^+$ T_H1-like response that may influence overall treatment efficacy in patients undergoing combination immunotherapy through modulation of the tumor-infiltrating myeloid compartment, including CD103$^+$ DCs.

Materials and Methods

Cell lines and mice

The C57BL/6 mouse breast carcinoma cell line AT-3ova^{dim} CD73$^+$ and the colon carcinoma line MC38ova^{dim} were generated as previously described and utilized within 3 weeks of thawing from a master stock generated in 2012 (31–33). United Kingdom Coordinating Committee on Cancer Research guidelines for the use of cell lines in cancer research were followed. Cells were not authenticated in the last year. Tumor lines were also verified to be *mycoplasma* negative by Victorian Infectious Diseases References Lab (Melbourne, Victoria) by PCR analysis. Tumor cells were grown in DMEM supplemented with 10% FCS, glutamax, and penicillin/streptomycin. For *in vivo* experiments, the indicated number of cells were resuspended in PBS and injected subcutaneously in a 100 μL volume. C57BL/6 WT and OTII mice were obtained from the Walter and Eliza Hall Institute of Medical Research (Melbourne), DEREG, IFNγ$^{-/-}$, and Batf3$^{-/-}$ mice were bred in house at the Peter MacCallum Cancer Centre, and IL12p35$^{-/-}$ or IL12p40$^{-/-}$ mice were either bred at the Peter MacCallum Cancer Centre or obtained from Prof. Hartland and Prof. van Driel (University of Melbourne).

Antibodies, cytokines, and peptides

Antibodies to PD-1 (RMP1-14), CTLA-4 (9H10), CD4 (GK1.5), or CD8α (YTS 169.4) IL12 p75 (R2-9A5) or isotype control (2A3) were purchased from Bio X Cell. IL2 used for T-cell stimulation was obtained from the National Institutes of Health (Bethesda, MD). $OVA_{323-339}$ peptide was purchased from GenScript.

Treatment of tumor-bearing mice

C57/BL6 mice were injected subcutaneously with 5×10^5 AT-3ova^{dim} CD73$^+$ or 1×10^6 MC38 ova^{dim} tumor cells. Once tumors were established (20–50 mm^2), mice were treated with either isotype control (2A3), anti–PD-1 (RMPI-14), or anti–CTLA-4 (9H10) with 3 to 4 doses given 4 days apart. For depletion of CD8$^+$ or CD4$^+$ cells, mice were dosed with the respective antibodies at 250 μg/mouse on days −1, 0, 4, 7, and 14 relative to treatment onset. Diptheria toxin (0.5 μg/mouse) was administered on the same days for the depletion of Foxp3$^+$ cells. For IL12 neutralization experiments, anti-IL12 was given on days −1, 0, and 4 prior to FACS analysis on day 7.

Analysis of tumor-infiltrating immune subsets

Seven days after treatment, tumors were excised and digested postmortem using a cocktail of 1 mg/mL collagenase type IV (Sigma-Aldrich) and 0.02 mg/mL DNase (Sigma-Aldrich). After digestion at 37°C for 30 minutes, cells were passed through a 70-μm filter twice. Inguinal lymph nodes were also harvested and cells were filtered through a 70-μm filter. Cells were then analyzed by flow cytometry as previously described (31) and Fixable Yellow (Thermo Fisher) used as a viability dye.

Intracellular cytokine staining

For detection of IFNγ production by T cells *ex vivo*, TILs and DLN cells were cultured for 3 hours with PMA (5 ng/mL) ionomycin (1 μg/mL) in the presence of GolgiPlug (BD Pharmingen) and GolgiStop (BD Pharmingen). After 3 hours, cells were analyzed by flow cytometry. For the detection of IL12p40, cells were cultured for 4 hours in GolgiPlug/GolgiStop either without further stimulation or with LPS (10 ng/mL).

Ex vivo culture of CD4$^+$ T cells derived from DLNs of tumor-bearing mice

Seven days after therapy onset, 2×10^5 cells derived from DLNs were cultured with 300 nmol/L $OVA_{323-339}$ peptide and IL2 for 5 days in a total volume of 200 μL. Supernatants were then taken for analysis of cytokine content by cytometric bead array.

Ex vivo assessment of antigen-presenting cells (APC) function of cells derived from DLNs of tumor-bearing mice

To assess the antigen-presenting function of cells derived from DLNs, 2×10^5 cells were irradiated (30 Gy) and then cultured with naïve splenocytes derived from OTII mice in the presence of 300 nmol/L $OVA_{323-339}$ peptide for 48 hours. Supernatants were then taken for analysis of cytokine content by cytometric bead array.

Statistical analysis

Statistical differences were analyzed by one-way or two-way ANOVA where indicated with $P < 0.05$ considered statistically significant.

Results

Induction of CD8$^+$/CD4$^+$ antitumor immune responses by dual PD-1/CTLA-4 blockade

We first evaluated the potential of monoclonal antibodies (mAb) to PD-1 and CTLA-4 to induce antitumor immune responses in a triple-negative breast cancer line AT-3ova^{dim}-CD73, a variant of AT-3ova^{dim} that is resistant to anti–PD-1 single-agent activity (31). Mice were injected with AT-3ova^{dim}-CD73 cells, and once tumors were established (20–50 mm^2), mice were treated with either isotype control (2A3), anti–PD-1, anti–CTLA-4, or a combination of both checkpoint inhibitors. Mice were treated with 4 doses of antibody, 4 days apart, and tumor growth and survival was monitored. The combination of PD-1 and CTLA-4 blockade significantly reduced tumor growth (Fig. 1A) and enhanced the survival of mice (Fig. 1B), whereas single blockade of either PD-1 or CTLA-4 had only modest antitumor activity. Similar results were obtained using the colon cancer cell line MC38 ova^{dim} (Fig. 1C and D).

To investigate the involvement of the CD4$^+$ and CD8$^+$ T-cell subsets in the antitumor immune response, mice bearing AT-3ova^{dim}-CD73 tumors were treated with anti–PD-1/anti–CTLA-4 in mice depleted of CD4$^+$ or CD8$^+$ T cells (Fig. 1E). Depletion of CD8$^+$ and CD4$^+$ T cells was effective, resulting in depletion of more than 90% of CD8$^+$ and CD4$^+$ T cells, respectively, as shown by FACS analysis of tumor-infiltrating lymphocytes at day 7 after treatment (Supplementary Fig. S1A–S1C). In the absence of therapeutic intervention, CD8$^+$ T-cell depletion had no significant effect on tumor outgrowth but significantly reduced the efficacy of anti–PD-1/anti–CTLA-4 combination therapy (Fig. 1E). In contrast, in the absence of checkpoint blockade, CD4$^+$ T-cell depletion resulted in decreased tumor growth, likely

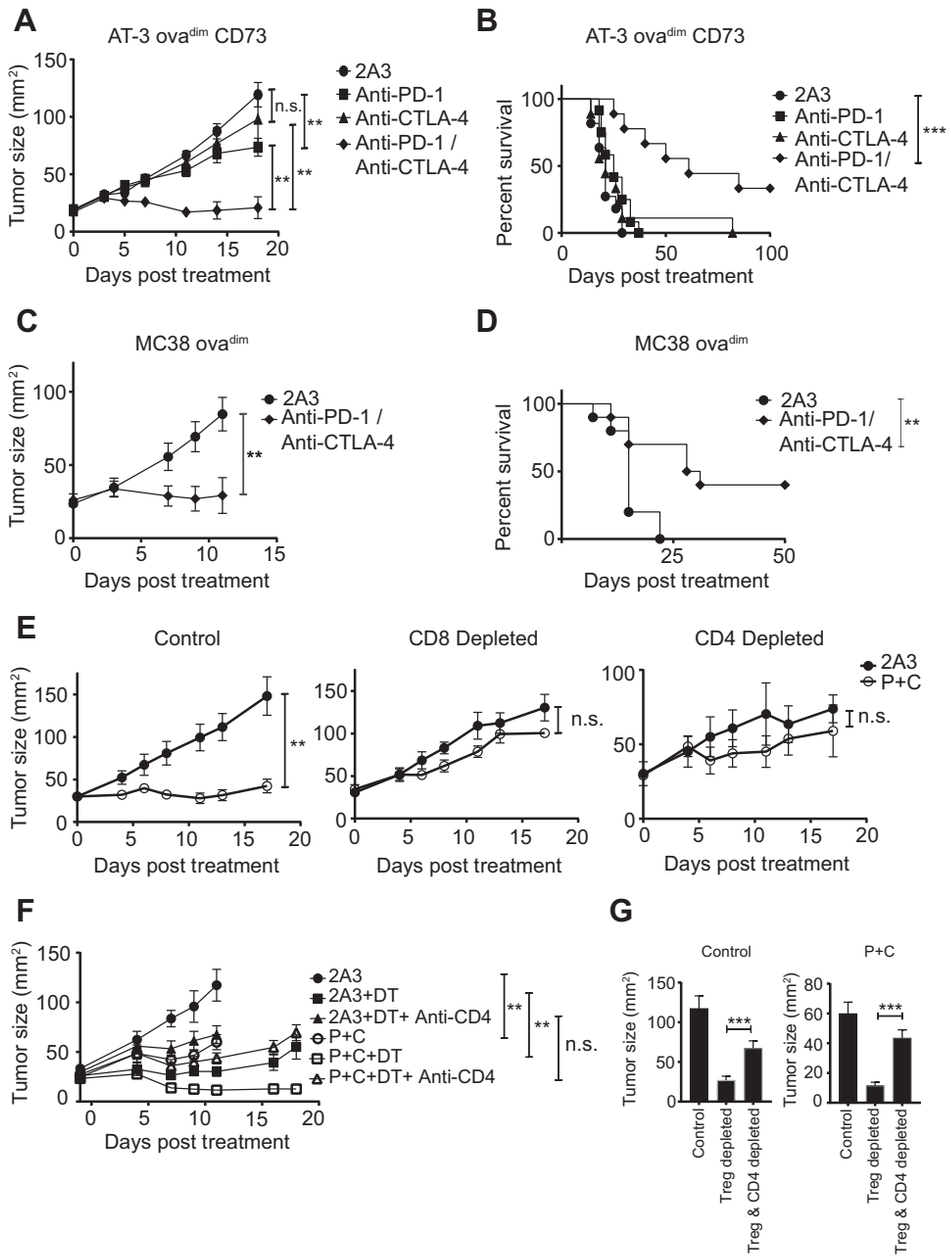

Figure 1.

Dual blockade of PD-1 and CTLA-4 results in robust antitumor immune responses. C57BL/6 WT (**A–E**) or DEREG (**F** and **G**) mice were injected s.c. with (**A, B, E–G**) 5×10^5 AT-3ova^{dim} CD73$^+$ cells or (**C** and **D**) 1×10^6 MC38 ova^{dim} tumor cells. Fourteen (**A–E**) or 17 (**F** and **G**) days after tumor inoculation, mice were treated with either anti–PD-1 (200 μg/mouse), anti–CTLA-4 (150 μg/mouse), isotype control (2A3; 200 μg/mouse) or a combination of anti–PD-1 and anti–CTLA-4 (P+C). Treatment was repeated on days 18, 22, and 26. **A, C, E,** Data shown as the mean ± SEM of 6 mice per group of a representative experiment ($n = 2$). **B** and **D,** Survival was determined as when tumor size exceeded 100 mm^2 $n = 9$–12 per group. **E,** On days 13, 14, and 21, mice were treated with either PBS, anti-CD4 (250 μg/mouse), or anti-CD8 (250 μg/mouse). **F** and **G,** Mice were treated on days 16, 17, and 21 with either PBS, anti-CD4 (250 μg/mouse) and/or diphtheria toxin (DT; 0.5 μg/mouse). **G,** Mean tumor size ± SEM at day 11 after treatment. Results shown as the mean ± SEM of 6–10 mice per group. **, $P < 0.01$; ***, $P < 0.001$; n.s., not significant (two-way ANOVA).

due to the depletion of CD4$^+$Foxp3$^+$ cells and the induction of an antitumor immune response. Treatment with anti–PD-1/anti–CTLA-4 did not further enhance the antitumor immune response in the context of CD4$^+$ T-cell depletion, suggesting that CD4$^+$Foxp3$^-$ T cells contribute to the efficacy of treatment following combination therapy. To further investigate the potential role of CD4$^+$Foxp3$^-$ cells in the therapeutic effect following dual PD-1/CTLA-4 blockade, we used DEREG mice, in which Foxp3$^+$ regulatory T cells (Treg) express a receptor for diphtheria toxin and so can specifically be depleted through the administration of diphtheria toxin. As expected, the depletion of Tregs led to a reduction in tumor growth and significantly enhanced the efficacy of anti–PD-1/anti–CTLA-4 therapy (Supplementary Fig. S1D and S1E; Fig. 1F). In this context, concurrent treatment with anti-CD4 (thus specifically depleting the CD4$^+$Foxp3$^-$ cells) significantly reduced the efficacy of combination treatment (Fig. 1F and G). Indeed, in the context of total CD4$^+$ depletion, anti–PD-1/anti–CTLA-4 did not significantly reduce tumor growth compared with 2A3 isotype–treated mice (Fig. 1F and G), consistent with our observations in wild-type mice (Fig. 1E). These data are therefore consistent with our hypothesis that CD4$^+$Foxp3$^-$ cells are required for the therapeutic efficacy of anti–PD-1/anti–CTLA-4.

Dual blockade of PD-1 and CTLA-4 activates both CD4$^+$Foxp3$^-$ and CD8$^+$ T cells

To investigate the mechanism by which dual blockade of PD-1 and CTLA-4 induces an antitumor immune response, we analyzed the phenotype of CD4$^+$Foxp3$^-$ and CD8$^+$ T cells isolated from the

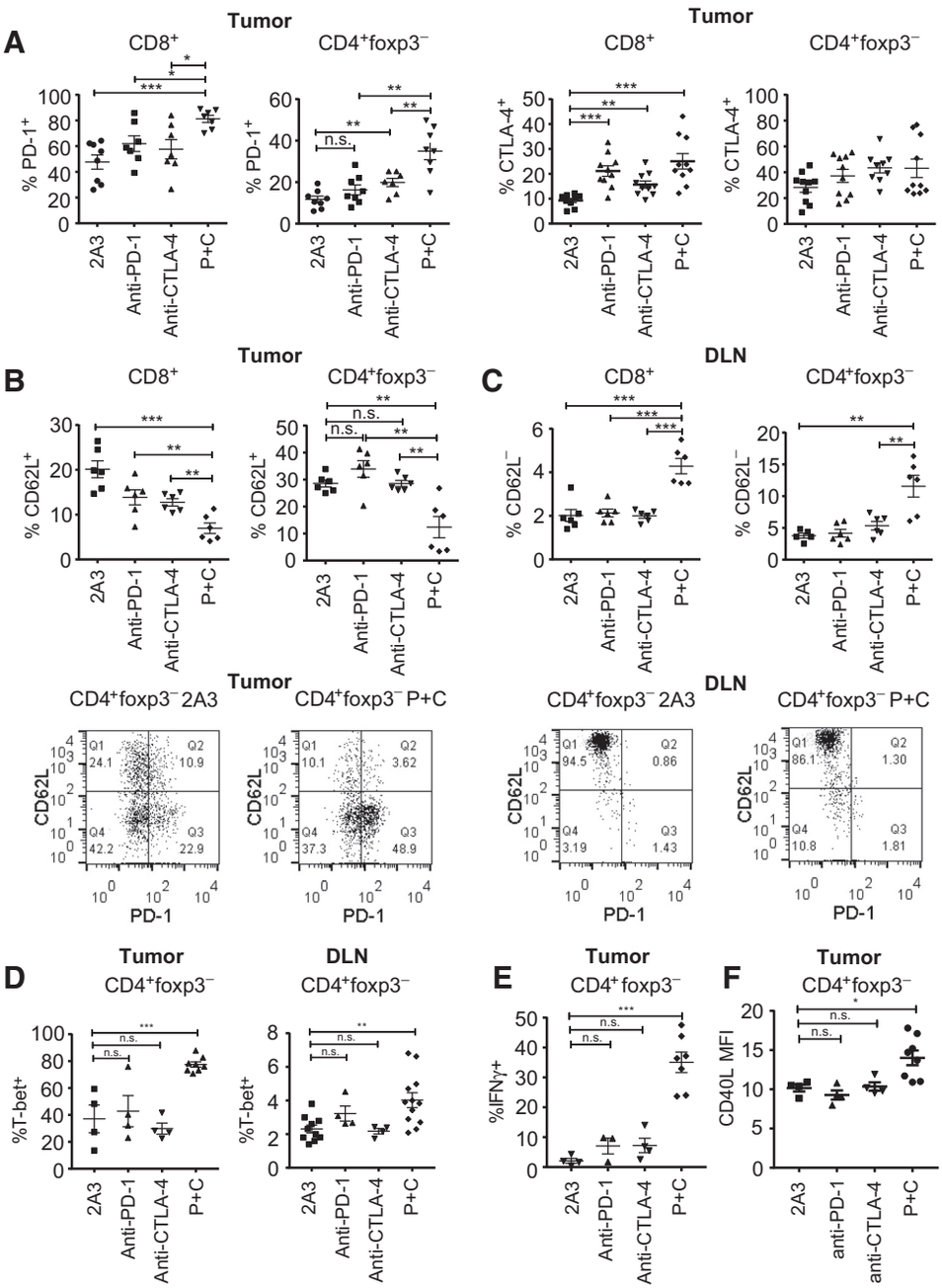

Figure 2.

Dual blockade of PD-1 and CTLA-4 results in the activation of both $CD8^+$ and $CD4^+Foxp3^-$ subsets. C57BL/6 mice were injected s.c. with 5×10^5 AT-3ova^{dim} $CD73^+$ tumor cells. Fourteen and 18 days after tumor inoculation, mice were treated with either anti–PD-1 (200 μg/mouse), anti–CTLA-4 (150 μg/mouse), isotype control (2A3; 200 μg/mouse), or a combination of anti–PD-1 and anti–CTLA-4 (P+C). On day 21 (7 days after treatment), $CD8^+$ and $CD4^+Foxp3^-$ cells from tumors (**A, B**, **D–F**) and DLNs (**C** and **D**) were analyzed by flow cytometry. Proportion of $CD8^+$ or $CD4^+Foxp3^-$ cells expressing PD-1, CTLA-4, CD62L, Tbet, IFNγ, and MFI of CD40L is shown. Data, mean ± SEM of 4–12 mice per group. **B** and **C,** Bottom, Representative flow cytometry plots are shown from concatenated samples. *, $P < 0.05$; **, $P < 0.01$; ***, $P < 0.001$; n.s., not significant (one-way ANOVA/Tukey).

tumors and DLNs of mice following combination therapy. Mice bearing AT-3ova^{dim}-CD73 tumors were treated with anti–PD-1 and anti–CTLA-4 as previously and tumor-infiltrating lymphocytes were analyzed at day 7 after therapy. The combination of anti–PD-1 and anti–CTLA-4 significantly enhanced the proportion of $CD8^+$ tumor-infiltrating T cells expressing PD-1, CTLA-4, and TIM-3 (Fig. 2A; Supplementary Fig. S2A). Similarly, combination therapy significantly increased the expression of PD-1 on

$CD4^+Foxp3^-$ cells and showed a trend for increased CTLA-4 expression on these cells (Fig. 2A). Combined PD-1 and CTLA-4 blockade also significantly reduced the proportion of both $CD8^+$ and $CD4^+Foxp3^-$ cells expressing CD62L in tumors (Fig. 2B) and DLNs (Fig. 2C), indicating a transition to an effector cell phenotype. Similarly, combination therapy significantly enhanced the expression of Tbet and IFNγ in $CD4^+Foxp3^-$ T cells isolated from tumors or DLNs (Fig. 2D and E; Supplementary Fig. S2B), the expression of CD40L on $CD4^+Foxp3^-$ TILs (Fig. 2F) as well as the proportion of $CD8^+$ TILs expressing granzyme B (Supplementary Fig. S2C). IFNγ is critical for the antitumor immune response evoked by PD-1 blockade (31), so we investigated the requirement for IFNγ in $CD4^+Foxp3^-$ and $CD8^+$ T-cell activation through the use of $IFN\gamma^{-/-}$ mice. This analysis revealed that IFNγ was critical for $CD4^+Foxp3^-$ and $CD8^+$ T-cell activation in the tumors, but not in the DLNs (Supplementary Fig. S2D).

Consistent with previous studies using the 9H10 clone of anti–CTLA-4 (18), treatment with anti–CTLA-4 alone, or the combination of anti–CTLA-4/anti–PD-1, resulted in a significant reduction in the proportion of $CD4^+Foxp3^+$ cells, and significantly enhanced the CD8:Treg and $CD4^+Foxp3^-$:Treg ratios (Supplementary Fig. S2E). Thus, dual blockade with anti–PD-1 and anti–CTLA-4 resulted in activation of both $CD8^+$ and $CD4^+Foxp3^-$ TILs and/or increased infiltration of activated $CD8^+$ and $CD4^+Foxp3^-$ cells. To confirm that these effects were broadly applicable, we also investigated the T-cell phenotype in MC38-ova^{dim} tumors treated with anti–PD-1 and/or anti–CTLA-4 (Supplementary Fig. S3). Similarly to the AT-3ova^{dim}-CD73 model, dual blockade of PD-1 and CTLA-4 resulted in significant activation of $CD4^+Foxp3^-$ cells. This was shown by increased expression of IFNγ within $CD4^+Foxp3^-$ cells isolated from tumors (Supplementary Fig. S3A) and $CD4^+Foxp3^-$ cells from DLNs exhibited an increased expression of IFNγ/Tbet and a transition toward an effector cell phenotype as shown by an enhanced proportion of $CD62L^-$ cells (Supplementary Fig. S3B).

Dual blockade of PD-1 and CTLA-4 results in direct activation of $CD4^+Foxp3^-$ cells

Given the significant activation of both $CD8^+$ and $CD4^+Foxp3^-$ cells in the tumors and DLNs following combination therapy, we next investigated whether $CD4^+Foxp3^-$ cells were activated directly by therapy, or whether their activation was an indirect consequence of modulation of $CD8^+$ and/or $CD4^+Foxp3^+$ cells. To investigate this, we first treated mice bearing established AT-3ova^{dim}-CD73 tumors with anti–PD-1/anti–CTLA-4 and compared the phenotype of $CD4^+Foxp3^-$ cells in control mice to those that had undergone CD8 depletion. As expected, combined PD-1 and CTLA-4 blockade activated $CD4^+Foxp3^-$ T cells as shown by the significant increase in Tbet expression (Fig. 3A), reduced proportion of $CD62L^+$ cells (Fig. 3B), and increased proportion of $IFN\gamma^+$ cells (Fig. 3C) in $CD4^{+-}Foxp3^-$ cells isolated from either tumors or DLNs. Surprisingly, in mice depleted of $CD8^+$ T cells, $CD4^+Foxp3^-$ cells were activated to a similar extent as in control mice, indicating that $CD8^+$ T cells were not required for the activation of $CD4^+Foxp3^-$ cells (Fig. 3A–C).

We next investigated a potential role for the modulation of $CD4^+Foxp3^+$ cells in this effect. This is particularly relevant because the 9H10 clone of anti–CTLA-4 depletes $CD4^+Foxp3^+$ Tregs (Supplementary Fig. S1D and S1E), which would consequently be expected to result in the activation of $CD4^+Foxp3^-$ cells by an indirect mechanism. To investigate this, we again utilized DEREG mice to specifically deplete $CD4^+Foxp3^+$ cells, thereby allowing investigation of the effect of anti–PD-1/anti–CTLA-4 therapy on $CD4^+Foxp3^-$ cells in the absence of $CD4^+Foxp3^+$ cells. Using this model, we concurrently depleted $CD8^+$ and $CD4^+Foxp3^+$ cells in mice bearing AT-3ova^{dim}-$CD73^+$ tumors. Therefore, in this setting, the only remaining αβ T lymphocyte population was $CD4^+Foxp3^-$ cells. Activation of $CD4^+Foxp3^-$ cells was then determined following dual PD-1/CTLA-4 blockade. Analysis of DLNs revealed that although Treg depletion in itself resulted in significant activation of $CD4^+Foxp3^-$ cells, anti–PD-1 and anti–CTLA-4 coblockade further enhanced the activation of $CD4^+Foxp3^-$ cells, as shown by significantly increased expression of Tbet (Fig. 3D), a decreased proportion of $CD62L^+$ cells (Fig. 3E), and significantly increased expression of IFNγ (Fig. 3F). Within the tumors, the expression of Tbet and IFNγ by $CD4^+Foxp3^-$ cells was also significantly increased by Treg depletion (Fig. 3D and F). No further increase in these parameters was observed following dual PD-1/CTLA-4 blockade, likely indicative of the highly activated state of these cells following Treg depletion. However, the proportion of $CD4^+Foxp3^-$ TILs expressing CD62L was significantly decreased (Fig. 3E), suggesting that $CD4^+Foxp3^-$ cells at the tumor site may still be directly modulated by PD-1/CTLA-4 dual blockade in the absence of $CD8^+$ and Treg populations. Thus, dual PD-1/CTLA-4 blockade resulted in robust activation of $CD4^+Foxp3^-$ cells in the absence of $CD8^+$ and $CD4^+Foxp3^+$ cells. Although we cannot formally exclude a role for other PD-1/CTLA-4 expressing cell types indirectly activating $CD4^+Foxp3^-$ cells, these data suggest that PD-1/CTLA-4 blockade can directly modulate $CD4^+Foxp3^-$ cells.

$CD4^+Foxp3^-$ cells modulate $CD103^+$ DCs following combination therapy

We next investigated the role of APCs in this effect and analyzed IL12 production *ex vivo* as a marker for APC activation. We analyzed the $CD11c^+$ compartment (Supplementary Fig. S4A) and observed that the production of IL12 was predominantly associated with the $CD103^+$ DC population (Supplementary Fig. S4B). The $CD103^+$ DCs produced significantly more IL12 than the $CD11b^+$, $CD11c^+$, and $CD11c^+CD103^-$ populations (Supplementary Fig. S4C), consistent with previous studies in which these cells were shown to secrete high levels of IL12, be highly effective at tumor-antigen presentation (26–28), and implicated in the therapeutic efficacy of checkpoint inhibition (29, 34). The anti–PD-1/anti–CTLA-4 combination therapy resulted in the activation of these cells, as shown by their enhanced IL12 production in both AT-3ova^{dim}-CD73 tumors (Fig. 4A) and MC38-ova^{dim} tumors (Supplementary Fig. S3C). The frequency of $CD11c^+CD103^+$ DCs within the DLNs increased with a concurrent reduction in the tumors following combination therapy, possibly representing DC egress following antigen uptake (Fig. 4B; Supplementary Fig. S3D) as has been reported previously (30). To investigate the role of $CD4^+Foxp3^-$ cells in the modulation of $CD103^+$ DC function and trafficking, we analyzed the effect of PD-1/CTLA-4 blockade in the context of CD8 and Treg depletion. These experiments revealed that even in the absence of $CD8^+$ and $CD4^+Foxp3^+$ cells, treatment of AT-3ova^{dim}-CD73 tumor–bearing mice with anti–PD-1/anti–CTLA-4 resulted in a significant increase in the proportion of $IL12^+$ $CD103^+CD11c^+$ DCs, implying a role for $CD4^+Foxp3^-$ cells in

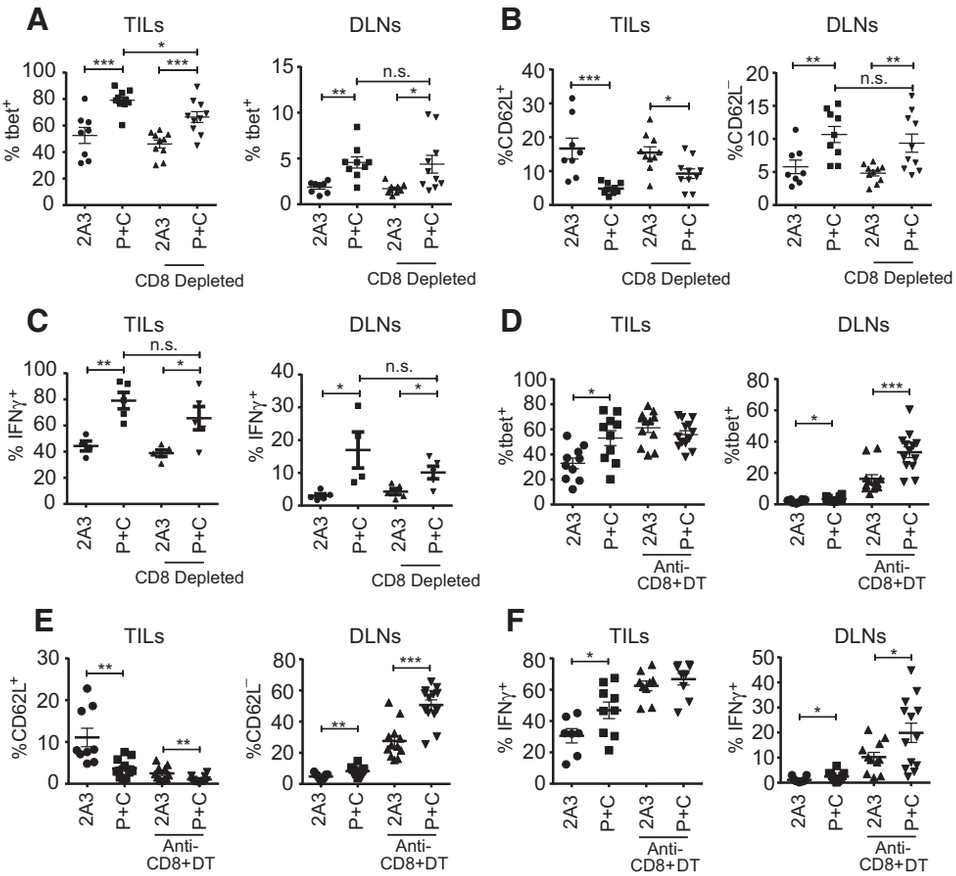

Figure 3.

Dual blockade of PD-1 and CTLA-4 directly activates $CD4^+Foxp3^-$ cells in the absence of $CD8^+$ or $CD4^+Foxp3^+$ cells. **A–C,** C57BL/6 WT or **D–F**. DEREG mice were injected s.c. with 5×10^5 AT-3ova^{dim} $CD73^+$ tumor cells. Mice were treated with 2A3 or anti–PD-1 and anti–CTLA-4 as per Fig. 2. On days 13, 14, and 18, mice were treated where indicated with anti-CD8 (250 μg/mouse) and/or diphtheria toxin (DT; 0.5 μg/mouse). On day 21, leukocytes were isolated from tumors (TILs) or DLNs and analyzed by flow cytometry. The expression of (**A, D**) Tbet, (**B, E**) CD62L, and (**C, F**) IFNγ by $CD4^+Foxp3^-$ cells was determined. Data shown as the mean ± SEM of 3–13 mice per group. *, $P < 0.05$; **, $P < 0.01$; ***, $P < 0.001$; n.s., not significant (one-way ANOVA/Tukey).

this response (Fig. 4C). Similarly, the increased frequency of $CD103^+CD11c^+$ DCs in the DLNs following dual PD-1/CTLA-4 blockade was not significantly affected by depletion of both $CD8^+$ and $CD4^+Foxp3^+$ T cells (Fig. 4D), and this was prevented by the concurrent depletion of the remaining $CD4^+(Foxp3^-)$ cells (Supplementary Fig. S4D), indicating the important role of $CD4^+$ $Foxp3^-$ cells in this effect.

To confirm the requirement of $CD103^+$ DCs for the therapeutic response, we investigated the efficacy of PD-1/CTLA-4 dual blockade in Batf3$^{-/-}$ mice. Combination therapy was ineffective in these mice, resulting in no enhancement of mouse survival (Fig. 4E) and an attenuated upregulation of Tbet and IFNγ in $CD4^+Foxp3^-$ T cells, compared with the effect observed in WT mice (Supplementary Fig. S4E). Supernatants collected from tumor samples cultured *ex vivo* contained no detectable IFNγ or TNFα from tumors grown in Batf3$^{-/-}$ mice, whereas these cytokines were significantly increased in tumors from WT mice treated with anti–PD-1/anti–CTLA-4 (Supplementary Fig. S4F). Thus, anti–PD-1/anti–CTLA-4 treatment enhanced IL12 production by $CD103^+$ DCs and increased their frequency in DLNs, even in the absence of $CD8^+$ and $CD4^+Foxp3^+$ T cells. This implied that activation of $CD4^+Foxp3^-$ T cells by the combination therapy was sufficient to trigger activation of $CD103^+$ DCs, possibly indicating direct modulation of these cells by $CD4^+Foxp3^-$ T cells.

$CD4^+Foxp3^-$ cell–mediated enrichment of a "TIP-DC" population following therapy

We further investigated the myeloid compartment of the tumor microenvironment (TME) following dual PD-1/CTLA-4 blockade, which revealed that treatment of AT-3ova^{dim}-CD73 tumor–bearing mice with anti–PD-1/anti–CTLA-4 combination therapy modulated a $CD11b^+Ly6C^{int}F4/80^+$ myeloid cell population within the tumors (Fig. 5A and B). Although neither anti–PD-1 nor anti–CTLA-4 modulated the proportion of these cells when given as a single therapy, dual blockade resulted in a significant increase in this subset (Fig. 5A and B). The enrichment of $CD11b^+Ly6C^{int}$ cells within the TME was dependent on T cells, because the frequency of these cells in RAG$^{-/-}$ mice treated with anti–PD-1/anti–CTLA-4 was not changed (Fig. 5C). Further phenotypic analysis showed that these cells were $MHCII^{high}CD86^+iNOS^+TNFα^+$, and a subset of these cells

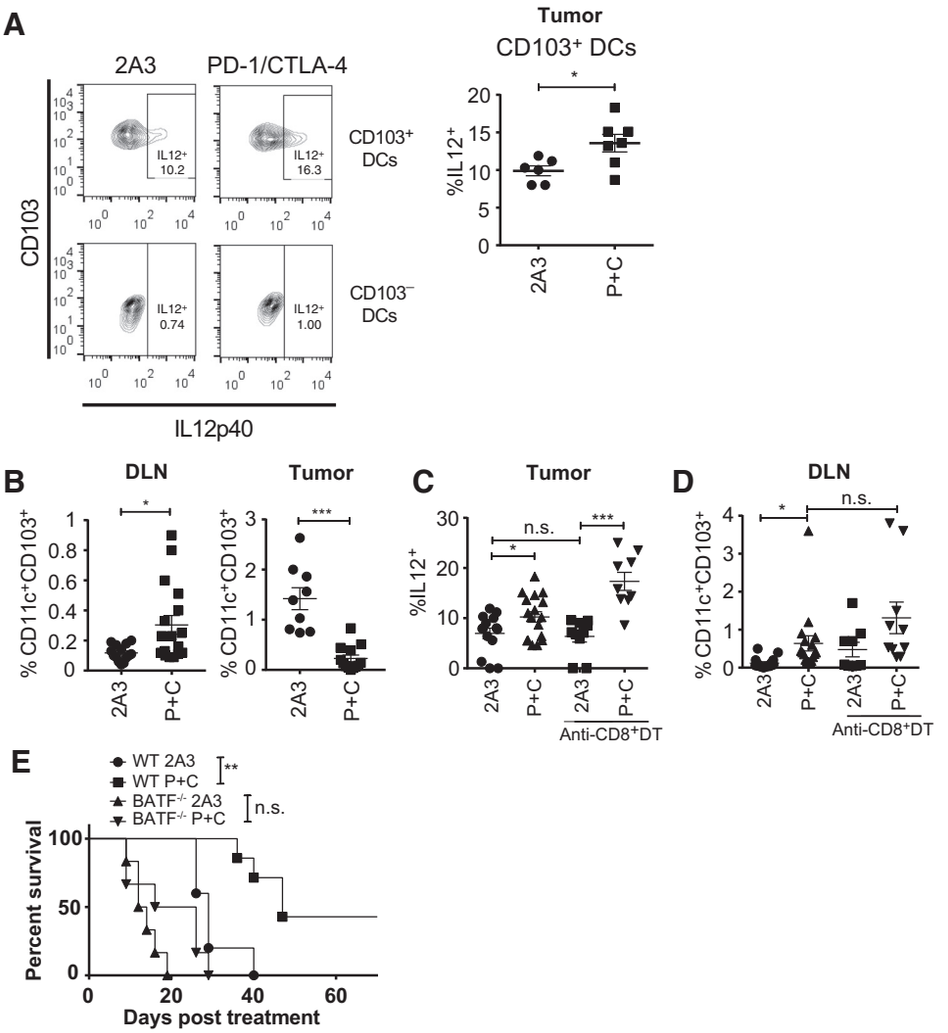

Figure 4.

Dual blockade of PD-1 and CTLA-4 results in the activation of CD103$^+$ DCs and their accumulation in DLNs. **A, B**, and **E,** C57BL/6 WT; **C–D,** DEREG, or **E**, Batf3$^{-/-}$ mice were injected s.c. with 5×10^5 AT-3ova^{dim} CD73$^+$ tumor cells. Mice were treated with 2A3 or anti–PD-1 and anti–CTLA-4 (P+C) and where indicated with anti-CD8 and diphtheria toxin (DT) as per Fig. 3. Seven days after treatment (**A–C**) tumor-infiltrating leukocytes and (**B, D**) DLNs were analyzed by flow cytometry. **A** and **C,** The proportion of CD103$^+$CD11c$^+$ (top) or CD103$^-$CD11c$^+$ (bottom) DCs expressing IL12 following a 4-hour incubation in GolgiPlug/GolgiStop. Right, Pooled data. **B, D,** The proportion of CD45$^+$ cells in the tumor or DLN that were CD103$^+$CD11c$^+$ DCs. **B–D,** Data are the mean ± SEM of 8–14 per group analyzed with a one-way ANOVA/Tukey test. **E,** Survival of mice is shown for $n = 5$–8 mice per group, with survival being determined as when tumors exceeded 100 mm^2. Statistical significance determined by Mantel–Cox test. *, $P < 0.05$; **, $P < 0.01$; ***, $P < 0.001$; n.s., not significant.

expressed CD11c and CXCR3 (Fig. 5D). The putative MDSC markers (35, 36) Ly6G, CD43, or CD115 were not detected on these cells (Fig. 5D). Thus, the phenotype of these cells was most consistent with the reported phenotype of TNFα and iNOS-producing DCs (TIP-DC; refs. 36–38). Although these cells are called "TIP-DCs," it has been suggested that these cells can be considered inflammatory macrophages (38). Further analysis of these cells after a cytospin revealed that these cells appeared macrophage-like in appearance, consistent with our hypothesis that they represent an inflammatory macrophage-like cell type (Fig. 5E).These CD11b$^+$Ly6C^{int}F4/80$^+$ cells are therefore herein referred to as "TIP-DCs."

Blockade of PD-1 and CTLA-4 significantly enhanced the proportion of TIP-DCs within tumors to a similar extent in the presence or absence of CD8$^+$ T cells (Fig. 5F) and was also observed in the context of CD8/Treg dual depletion (Fig. 5G). However, CD4$^+$ T-cell depletion ablated the increased frequency of TIP-DCs following anti–PD-1/anti–CTLA-4 treatment of mice depleted of both CD8$^+$ T cells and CD4$^+$Foxp3$^+$ cells, showing the importance of the CD4$^+$Foxp3$^-$ cells in this effect (Fig. 5G). A minor population of TIP-DCs expressed CD4, but most were CD4 negative, indicating that direct depletion of TIP-DCs following anti-CD4 treatment could not fully account for this effect (Supplementary Fig. S5).

Enhanced CD4$^+$ T-cell activation and APC function in DLNs after dual blockade

Due to the increased frequency of CD103$^+$ DCs observed in DLNs following PD-1/CTLA-4 blockade, we hypothesized that this would lead to enhanced APC function. To investigate this, we assessed CD4$^+$ T cell and APC function in cells isolated from the DLNs of anti–PD-1/anti–CTLA-4-treated mice or 2A3 isotype control in both control mice and those treated in the context of CD8 depletion.

To evaluate the functional consequences of PD-1/CTLA-4 blockade on CD4$^+$ T cells, we evaluated the *ex vivo* cytokine production of CD4$^+$ T cells isolated from the DLNs of AT-3ova^{dim}-CD73 tumor–bearing mice. DLN cells were isolated and stimulated with 300 nmol/L of the ovalbumin MHCII-restricted peptide OVA$_{323\text{-}339}$ and IL2. After 5 days of culture, cytokine production was analyzed. In this setting, treatment of mice with PD-1/CTLA-4 significantly increased the production of IFNγ and TNFα, but not IL17 (Fig. 6A). The DLN cells isolated from mice depleted of CD8$^+$ T cells produced

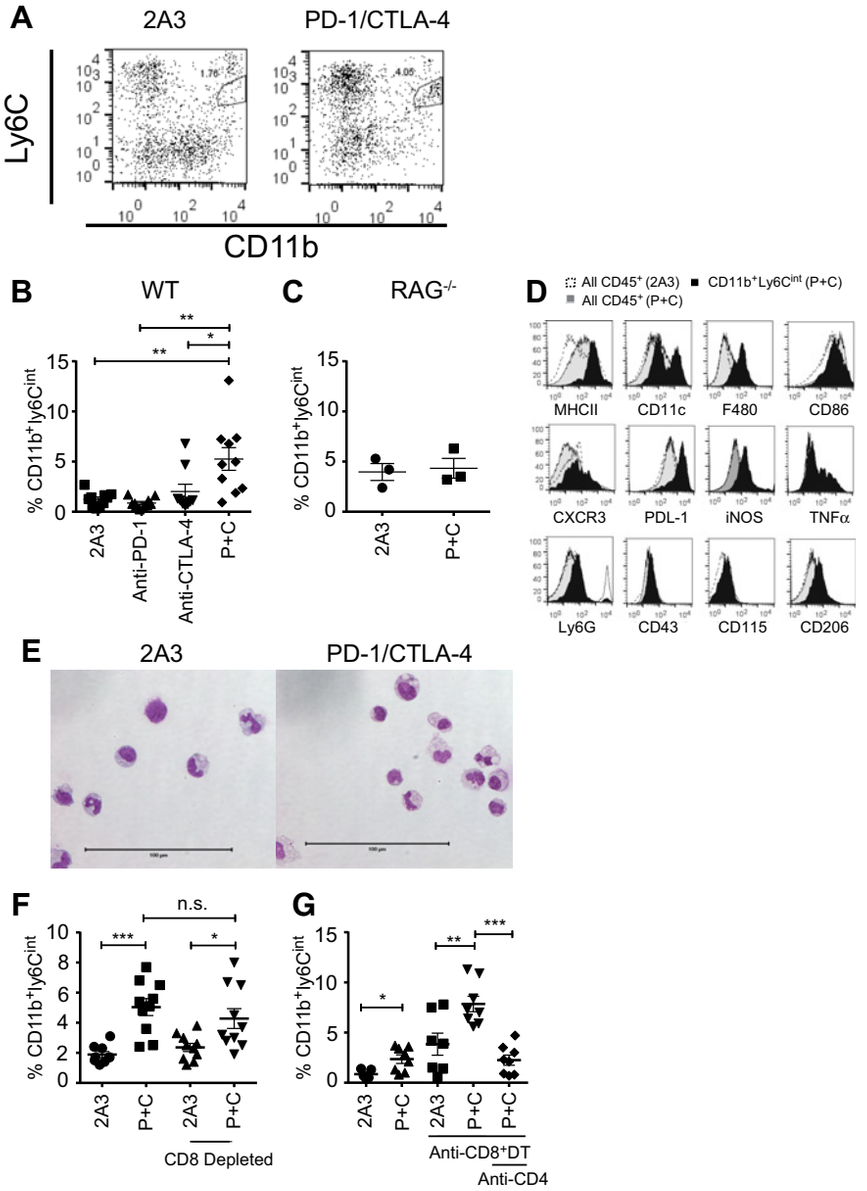

Figure 5.

Dual blockade of PD-1 and CTLA-4 results in an enrichment of CD11b$^+$Ly6C^{int} TIP-DCs in a CD4$^+$ T cell–dependent manner. **A, B**, and **D–F,** C57BL/6 WT; **C**, RAG$^{-/-}$; or **G,** DEREG mice were injected s.c. with 5 $\times$ 10^5 AT-3ova^{dim} CD73$^+$ tumor cells. Mice were treated with either isotype control (2A3; 200 μg/mouse) or a combination of anti–PD-1 (200 μg/mouse) and/or anti–CTLA-4 (150 μg/mouse; P+C) and where indicated with anti-CD8 (250 μg/mouse), anti-CD4 (250 μg/mouse), and/or diphtheria toxin (DT; 0.5 μg/mouse) as per Fig. 3. On day 21, leukocytes were isolated from tumors and analyzed by flow cytometry or morphology assessed following cytospin. **A–C, F, G,** The percentage of tumor-infiltrating CD11b$^+$Ly6C^{int} cells as a proportion of CD45$^+$ live cells. **A**. Representative FACS plot from 5 concatenated samples. **B–C, F, G,** Data shown as the mean ± SEM of 3–10 mice per group. **D,** Expression of indicated markers on all CD45$^+$ cells (dashed histograms), all CD45$^+$ cells following combination therapy (gray histograms) and on CD11b$^+$Ly6C^{int} cells following combination therapy (black histograms). **E,** Cytospin of CD11b$^+$Ly6C^{int} cells following combination therapy. *, $P < 0.05$; **, $P < 0.01$; ***, $P < 0.001$; n.s., not significant (one-way ANOVA/Tukey).

equivalent amounts of these cytokines following anti–PD-1/anti–CTLA-4 treatment (Fig. 6A). Thus, increased CD4$^+$ T-cell cytokine production was achieved independently of CD8$^+$ T cells, suggestive of direct modulation of this subset by anti–PD-1/anti–CTLA-4.

Given our previous observations concerning the CD4$^+$Foxp3$^-$ T cell–dependent enrichment of CD103$^+$ DCs in the DLNs following PD-1/CTLA-4 blockade (Fig. 4), we next investigated the antigen-presentation function of DLN cells isolated from mice bearing AT-3ova^{dim}-CD73 tumors. DLN cells were irradiated (30 Gy) and then cocultured with naïve OTII cells in the presence of 300 nmol/L of the OTII specific OVA$_{323-339}$ peptide. After 48 hours, supernatants were harvested and concentrations of IFNγ, IL2, TNFα, and IL17 were determined. DLNs isolated from mice treated with anti–PD-1/anti–CTLA-4 induced significantly higher amounts of IFNγ, IL2, TNFα, and IL17 (Fig. 6B). CD8$^+$ T-cell depletion did not significantly affect this enhanced APC capacity of DLNs, suggesting that direct modulation of the CD4$^+$ population by PD-1/CTLA-4 blockade was sufficient to enhance APC functional activity. Thus, combined PD-1/CTLA-4 blockade results in direct activation of CD4$^+$ T cells and consequent licensing of APCs within DLNs, which further promotes CD4$^+$ T-cell responses to tumor antigens at this site.

Activation of CD4$^+$ T cells by dual PD-1/CTLA-4 blockade is partly IL12 dependent

Having shown that combined PD-1/CTLA-4 blockade resulted in enhanced IL12 production of tumor-infiltrating CD103$^+$ DCs, we next investigated the significance of IL12 in the therapeutic effect. The growth of AT-3ova^{dim}-CD73 tumors in WT and IL12p35$^{-/-}$ mice following treatment with anti–PD-1/anti–CTLA-4 or isotype control was compared. Although the initial

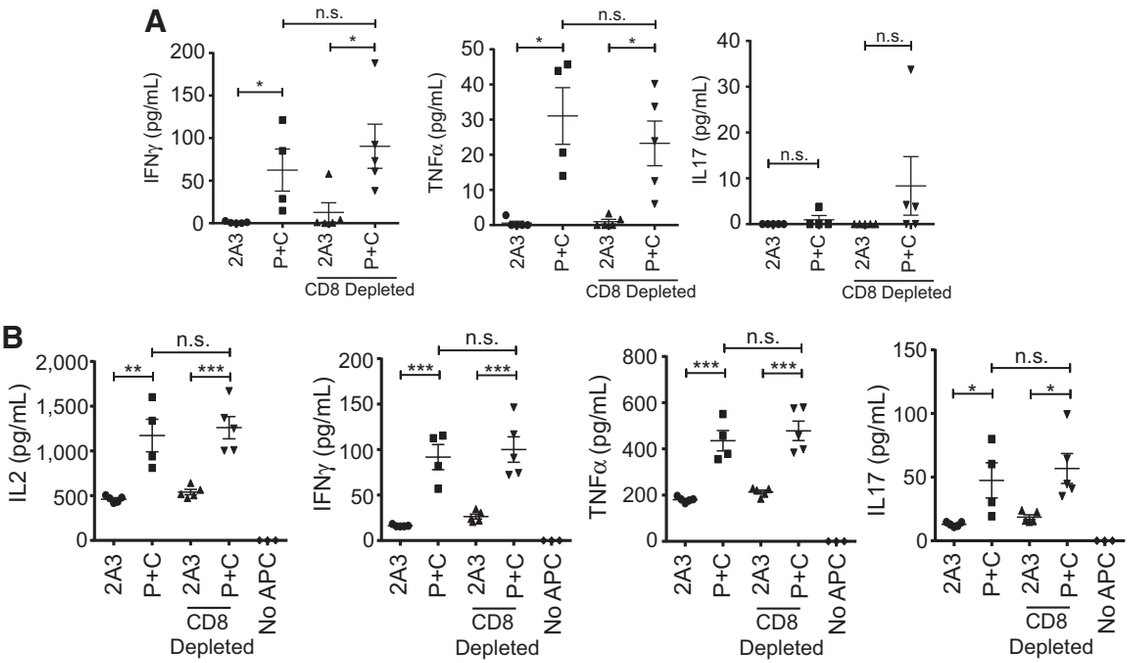

Figure 6.

Dual blockade of PD-1 and CTLA-4 directly activates $CD4^+$ T cells resulting in enhanced APC function in DLNs and enhanced tumor-antigen-specific responses. C57BL/6 WT mice were injected s.c. with 5×10^5 AT-3ova^{dim} $CD73^+$ tumor cells and treated with 2A3 or anti–PD-1 and anti–CTLA-4 and in some cases anti-CD8 depletion antibody as per Fig. 3. On day 21, leukocytes were isolated from DLNs (DLNs). **A,** 2×10^5 lymph node cells were stimulated for 5 days with 300 nmol/L $OVA_{323–339}$ peptide and IL2 (100 IU/mL). **B,** 2×10^5 lymph node cells were irradiated (30 Gy) and cocultured with naïve OTII splenocytes (2×10^5) for 48 hours. **A** and **B,** Cytokine concentration was determined by cytometric bead array. Data are shown as the mean SEM of 4–5 mice per group from a representative experiment of $n = 2$. *, $P < 0.05$; **, $P < 0.01$; ***, $P < 0.001$; n.s., not significant (one-way ANOVA/Tukey).

antitumor effect mediated by dual blockade was similar in WT and IL12 $p35^{-/-}$ mice, tumors outgrew significantly faster in IL12 $p35^{-/-}$ mice, resulting in a significantly longer survival of WT mice compared with IL12 $p35^{-/-}$ mice (Fig. 7A). As the p35 subunit of IL12 is also expressed by IL35, we confirmed this effect using IL12 $p40^{-/-}$ mice. IL12$p40^{-/-}$ mice showed a similar phenotype to IL12$p35^{-/-}$ mice with regard to a less potent antitumor immune response (Fig. 7B), thus confirming the role of IL12 in this response. To investigate the underlying mechanism in this effect, we analyzed the phenotype of tumor-infiltrating T cells. In wild-type mice, as expected, anti–PD-1/anti–CTLA-4 induced robust $CD4^+Foxp3^-$ T-cell activation (Fig. 7C). However, in IL12$p35^{-/-}$ mice, we observed that the ability of anti–PD-1/anti–CTLA-4 treatment to induce Tbet expression and IFNγ production by $CD4^+Foxp3^-$ cells was significantly reduced (Fig. 7C). Similarly, IL12 neutralization with anti-IL12p75 reduced the expression of Tbet in tumor-infiltrating $CD4^+Foxp3^-$ cells, confirming that $CD4^+$Foxp3 T-cell activation following dual PD-1/CTLA-4 blockade was partly IL12 dependent (Fig. 7D). Although there was no significant induction of $tbet^+$ cells in IL12$p35^{-/-}$ mice (Fig. 7C), a significant increase was observed in the context of IL12p70 neutralization (Fig. 7D), albeit to a lesser extent than in WT mice. These differences are potentially explained by incomplete neutralization of IL12 in these experiments. In contrast to effects observed with $CD4^+$ T cells, the induction of IFNγ by $CD8^+$ T cells was not significantly different in IL12$p35^{-/-}$ mice compared with wild-type mice (Fig. 7E). Taken together, our data indicate that the activation of $CD4^+Foxp3^-$ cells following checkpoint blockade results in the modulation of $CD103^+$ DCs to secrete more IL12, which plays an important role in the antitumor response (Supplementary Fig. S6).

Discussion

Our understanding of the mechanism by which anti–PD-1 and anti–CTLA-4 evoke antitumor immune responses is incomplete, and prognostic markers that can predict responses to checkpoint inhibitors are lacking. Our current study reveals that the interplay between $CD4^+Foxp3^-$ T cells and $CD103^+$ DCs may be crucial in the antitumor immune response evoked by dual blockade of PD-1 and CTLA-4.

The original description of the efficacy of dual PD-1/CTLA-4 blockade by Jim Allison's group revealed that this therapeutic combination resulted in the activation of both $CD8^+$ and $CD4^+$ T cells (24). Further studies have shown that CTLA-4 blockade modulates both Treg and non-Treg compartments (18, 39, 40), although none of these studies could exclude the possibility that anti–CTLA-4 activates $CD4^+Foxp3^-$ cells indirectly through modulation of $CD8^+$ or $Foxp3^+$ T cells. In patients, it has been observed that the $CD4^+$ T-cell compartment becomes activated following immunotherapy with checkpoint inhibitors including anti–PD-1 and anti–CTLA-4 combination therapy (13, 41–43). Furthermore, neoantigen-specific $CD4^+$ T cells that may be responsive to immunotherapy have been observed in patients with cancer (20–23), and thus robust activation of tumor-antigen

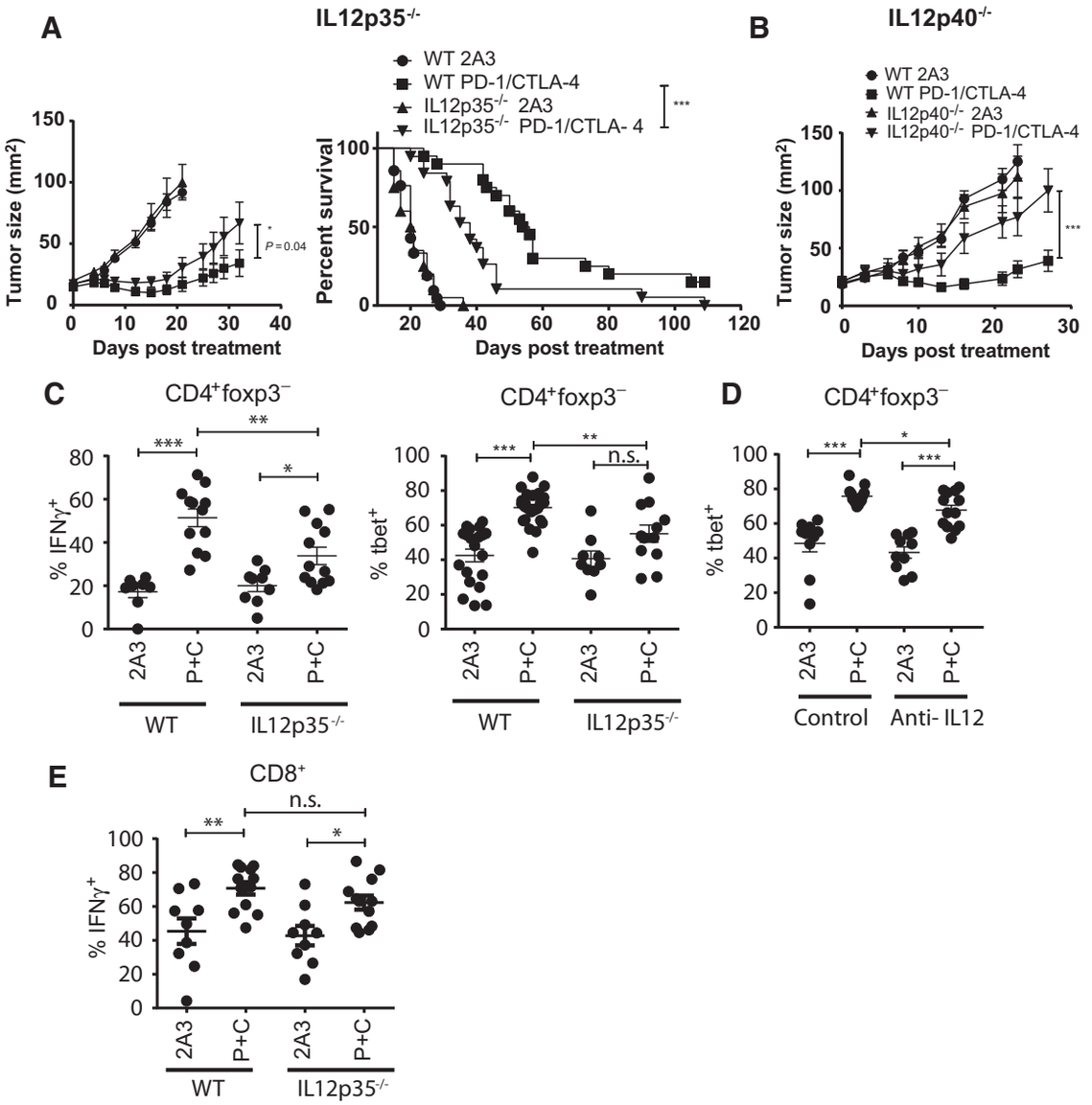

Figure 7.

Activation of $CD4^+Foxp3^-$ cells and therapeutic activity of anti–PD-1/anti–CTLA-4 combination therapy is partly IL12 dependent. **A–E,** C57BL/6 WT; **A, C, E,** IL12p35$^{-/-}$; or **B,** IL12p40$^{-/-}$ mice were injected s.c. with 5×10^5 AT-3ova^{dim} $CD73^+$ tumor cells and treated with 2A3 or anti–PD-1 and anti–CTLA-4 (P+C) as per Fig. 3. **A** and **B,** Tumor growth and survival of WT, IL12 p35$^{-/-}$, and IL12p40$^{-/-}$ mice. Tumor growth data are shown as the mean ± SEM of 7–8 mice per group from a representative experiment, and survival, determined as when tumor size exceeded 100 mm^2, of $n = 7$–21 per group from pooled experiments is shown. Statistical test: two-way ANOVA/Mantel–Cox test. **C–E,** On day 21, leukocytes were isolated from tumors and analyzed by flow cytometry. **D,** Where indicated mice were treated with 500 μg per mouse anti-IL12 (R2-9A5) on days 13, 14, and 18. Expression of IFNγ and Tbet in **C–D**, $CD4^+Foxp3^-$ and **E,** $CD8^+$ T cells is shown. Data, mean ± SEM of 8–25 mice per group. *, $P < 0.05$; **, $P < 0.01$; ***, $P < 0.001$; n.s., not significant (one-way ANOVA/Tukey).

specific $CD4^+$ T cells is likely to be important for optimal therapeutic efficacy. However, the importance of $CD4^+Foxp3^-$ cells in response to PD-1 and CTLA-4 is currently not fully understood.

Our study revealed that $CD4^+Foxp3^-$ cells were robustly activated by the combination of anti–PD-1 and anti–CTLA-4. This led to the increased expression of CD40L, Tbet, and IFNγ in $CD4^+Foxp3^-$ cells isolated from tumors and DLNs, in part due to a direct activation of these $CD4^+Foxp3^-$ cells. This activation of $CD4^+Foxp3^-$ cells was sufficient to induce an enhanced proportion of a myeloid cell with a phenotype consistent with previously reported TNFα, iNOS-producing DCs (TIP-DC; refs. 36–38). Although the functional importance of these cells remains to be determined, these TIP-DCs may be capable of modulating T-cell responses at the tumor site through antigen presentation (44, 45) or conversely through the iNOS-mediated suppression (46).

Activation of $CD4^+Foxp3^-$ cells was sufficient to induce the activation of tumor-residing $CD103^+$ DCs, even in the absence of $CD8^+$ and $CD4^+Foxp3^+$ cells, highlighting an interaction

between T_H1 effector cells and $CD103^+$ DCs. $CD103^+$ DCs are highly efficient at tumor-antigen presentation (26, 28, 47) and have been shown to enhance the therapeutic activity of anti–PDL-1/BRAF inhibition (29) or anti-TIM3 (48). $CD103^+$ DCs are thus likely to play a critical role in the therapeutic responses to checkpoint inhibitors. Our study shows that combining PD-1 and CTLA-4 blockade induces $CD103^+$ DCs to produce IL12, in part through the activation of $CD4^+Foxp3^-$ cells, which contributed to the therapeutic effect of the combination therapy. The $CD103^+$ DCs were the highest per cell producers of IL12p40 in the tumor microenvironment following dual PD-1/CTLA-4 blockade, consistent with previous publications showing that $CD103^+$ DCs were the major producers of IL12 in the tumor microenvironment following paclitaxel therapy (27) and that the production of IL12 by Batf3-dependent DCs enhances NK cell–mediated antimetastatic effects (49). IL12 is required for the antitumor effect of CpG (50) and anti-CD40 (51) and here we demonstrate the importance of IL12 in the context of checkpoint inhibition. We observed that IL12 production was particularly important for long-term antitumor immune responses. Thus, the activation of $CD103^+$ DCs by $CD4^+Foxp3^-$ cells may contribute to memory T-cell responses. $CD8^+$ memory formation is most efficient when $CD4^+$ and $CD8^+$ cells recognize cognate antigen on the same APC (52–54), and our data imply that this mechanism may be leading to more robust antitumor $CD8^+$ T-cell activity in our system.

The increased frequency of $CD103^+$ DCs in the DLNs following PD-1/CTLA-4 dual blockade could represent enhanced trafficking of these cells from the tumor site and transfer of tumor antigens to lymph node residing APCs, as observed by Krummel and colleagues (30). Taken together, our data highlight the importance of $CD4^+Foxp3^-$ cells in the activation and migration of these cells.

In summary, our data show that $CD4^+Foxp3^-$ cells can be activated by dual PD-1/CTLA-4 blockade in the absence of $CD8^+$ and $CD4^+Foxp3^+$ cells, inferring a direct activation of $CD4^+Foxp3^-$ cells. This activation was sufficient to induce the activation of $CD103^+$ DCs as shown by their enhanced IL12 production. In turn, IL12 production following anti–PD-1/anti–CTLA-4 was required for optimal $CD4^+Foxp3^-$ cell activation and therapeutic activity. These data are consistent with the observation that PD-1 and CTLA-4 blockade activate distinct transcriptional pathways in $CD4^+$ T cells in treated mice and that the induction of a $CD4^+PD\text{-}1^{hi}Tbet^+$ population negatively correlated with tumor growth (55). Our data revealed an additional mechanism by which $CD4^+Foxp3^-$ cell activation contributes to the overall efficacy of checkpoint inhibition.

Disclosure of Potential Conflicts of Interest

S. Loi reports receiving a commercial research grant from Bristol-Myers Squibb and Merck, reports receiving other commercial research support from Novartis, Roche-Genentech, and Pfizer, and is a consultant/advisory board member for Bristol-Myers Squibb, Merck, Roche-Genentech, Puma Biotechnology, Novartis, Seattle Genetics, and Pfizer. No potential conflicts of interest were disclosed by the other authors.

Authors' Contributions

Conception and design: P.A. Beavis, C.Y. Slaney, J.A. Trapani, P.K. Darcy
Development of methodology: P.A. Beavis, C.Y. Slaney, J.A. Trapani, P.K. Darcy
Acquisition of data (provided animals, acquired and managed patients, provided facilities, etc.): P.A. Beavis, M.A. Henderson, L. Giuffrida, A.J. Davenport, E.V. Petley, I.G. House, J. Lai, K. Sek, N. Milenkovski, S. Mardiana, C.Y. Slaney, S. Loi, P.K. Darcy
Analysis and interpretation of data (e.g., statistical analysis, biostatistics, computational analysis): P.A. Beavis, M.A. Henderson, L. Giuffrida, A.J. Davenport, E.V. Petley, K. Sek, S. Loi, M.H. Kershaw, P.K. Darcy
Writing, review, and/or revision of the manuscript: P.A. Beavis, M.A. Henderson, E.V. Petley, I.G. House, J. Lai, J.A. Trapani, S. Loi, M.H. Kershaw, N.M. Haynes, P.K. Darcy
Administrative, technical, or material support (i.e., reporting or organizing data, constructing databases): M.A. Henderson, L. Giuffrida, K. Sek, N. Milenkovski, L.B. John, P.K. Darcy
Study supervision: P.A. Beavis, J.A. Trapani, P.K. Darcy

Acknowledgments

This work was funded by a Project and Program Grant from the National Health and Medical Research Council (NHMRC; grant number 1062580), a Cancer Council Victoria Project Grant (APP1084420), and a grant from the Peter MacCallum Cancer Centre Foundation. P.A. Beavis and C.Y. Slaney are supported by National Breast Cancer Foundation Fellowships (ID# ECF-17-005 and #ECF-16-005). P.K. Darcy and M.H. Kershaw are supported by NHMRC Senior Research Fellowships (APP1041828 and APP1058388, respectively).

The authors would like to acknowledge the assistance of the Animal Facility Technicians at the Peter MacCallum Cancer Centre. We also thank Prof. Hartland, Prof. van Driel and Garrett Ng (University of Melbourne) for the provision of $IL12p35^{-/-}$ and $IL12p40^{-/-}$ mice. We also thank and acknowledge Dr. Trina Stewart (Griffith University, Queensland) who originally generated the AT-3 tumor cell line.

The costs of publication of this article were defrayed in part by the payment of page charges. This article must therefore be hereby marked *advertisement* in accordance with 18 U.S.C. Section 1734 solely to indicate this fact.

Received May 2, 2018; revised July 9, 2018; accepted July 10, 2018; published first July 17, 2018.

References

1. Galon J, Costes A, Sanchez-Cabo F, Kirilovsky A, Mlecnik B, Lagorce-Pages C, et al. Type, density, and location of immune cells within human colorectal tumors predict clinical outcome. Science 2006;313:1960–4.
2. Dushyanthen S, Beavis PA, Savas P, Teo ZL, Zhou C, Mansour M, et al. Relevance of tumor-infiltrating lymphocytes in breast cancer. BMC Med 2015;13:202.
3. Loi S, Sirtaine N, Piette F, Salgado R, Viale G, Van Eenoo F, et al. Prognostic and predictive value of tumor-infiltrating lymphocytes in a phase III randomized adjuvant breast cancer trial in node-positive breast cancer comparing the addition of docetaxel to doxorubicin with doxorubicin-based chemotherapy: BIG 02–98. J Clin Oncol 2013;31:860–7.
4. Brahmer JR, Tykodi SS, Chow LQ, Hwu WJ, Topalian SL, Hwu P, et al. Safety and activity of anti-PD-L1 antibody in patients with advanced cancer. N Engl J Med 2012;366:2455–65.
5. Zou W, Wolchok JD, Chen L. PD-L1 (B7-H1) and PD-1 pathway blockade for cancer therapy: mechanisms, response biomarkers, and combinations. Sci Transl Med 2016;8:328rv4.
6. Buchbinder EI, Desai A. CTLA-4 and PD-1 pathways: similarities, differences, and implications of their inhibition. Am J Clin Oncol 2016;39:98–106.
7. Schadendorf D, Hodi FS, Robert C, Weber JS, Margolin K, Hamid O, et al. Pooled analysis of long-term survival data from phase II and phase III trials of ipilimumab in unresectable or metastatic melanoma. J Clin Oncol 2015;33:1889–94.
8. Boutros C, Tarhini A, Routier E, Lambotte O, Ladurie FL, Carbonnel F, et al. Safety profiles of anti-CTLA-4 and anti-PD-1 antibodies alone and in combination. Nat Rev Clin Oncol 2016;13:473–86.
9. Pardoll DM. The blockade of immune checkpoints in cancer immunotherapy. Nat Rev Cancer 2012;12:252–64.

10. Carlino MS, Long GV. Ipilimumab combined with nivolumab: a standard of care for the treatment of advanced melanoma? Clin Cancer Res 2016;22:3992–8.
11. Twyman-Saint Victor C, Rech AJ, Maity A, Rengan R, Pauken KE, Stelekati E, et al. Radiation and dual checkpoint blockade activate non-redundant immune mechanisms in cancer. Nature 2015;520:373–7.
12. Choudhury N, Nakamura Y. Importance of immunopharmacogenomics in cancer treatment: patient selection and monitoring for immune checkpoint antibodies. Cancer Sci 2016;107:107–15.
13. Das R, Verma R, Sznol M, Boddupalli CS, Gettinger SN, Kluger H, et al. Combination therapy with anti-CTLA-4 and anti-PD-1 leads to distinct immunologic changes in vivo. J Immunol 2015;194:950–9.
14. Taube JM, Klein A, Brahmer JR, Xu H, Pan X, Kim JH, et al. Association of PD-1, PD-1 ligands, and other features of the tumor immune microenvironment with response to anti-PD-1 therapy. Clin Cancer Res 2014;20:5064–74.
15. Herbst RS, Soria JC, Kowanetz M, Fine GD, Hamid O, Gordon MS, et al. Predictive correlates of response to the anti-PD-L1 antibody MPDL3280A in cancer patients. Nature 2014;515:563–7.
16. Tumeh PC, Harview CL, Yearley JH, Shintaku IP, Taylor EJ, Robert L, et al. PD-1 blockade induces responses by inhibiting adaptive immune resistance. Nature 2014;515:568–71.
17. Gajewski TF, Fallarino F, Fields PE, Rivas F, Alegre ML. Absence of CTLA-4 lowers the activation threshold of primed CD8+ TCR-transgenic T cells: lack of correlation with Src homology domain 2-containing protein tyrosine phosphatase. J Immunol 2001;166:3900–7.
18. Simpson TR, Li F, Montalvo-Ortiz W, Sepulveda MA, Bergerhoff K, Arce F, et al. Fc-dependent depletion of tumor-infiltrating regulatory T cells co-defines the efficacy of anti-CTLA-4 therapy against melanoma. J Exp Med 2013;210:1695–710.
19. Arce Vargas F, Furness AJS, Litchfield K, Joshi K, Rosenthal R, Ghorani E, et al. Fc effector function contributes to the activity of human anti-CTLA-4 antibodies. Cancer Cell 2018;33:649–63e4.
20. Linnemann C, van Buuren MM, Bies L, Verdegaal EM, Schotte R, Calis JJ, et al. High-throughput epitope discovery reveals frequent recognition of neo-antigens by CD4+ T cells in human melanoma. Nat Med 2015;21:81–5.
21. Kreiter S, Vormehr M, van de Roemer N, Diken M, Lower M, Diekmann J, et al. Mutant MHC class II epitopes drive therapeutic immune responses to cancer. Nature 2015;520:692–6.
22. Tran E, Turcotte S, Gros A, Robbins PF, Lu YC, Dudley ME, et al. Cancer immunotherapy based on mutation-specific CD4+ T cells in a patient with epithelial cancer. Science 2014;344:641–5.
23. Verdegaal EM, de Miranda NF, Visser M, Harryvan T, van Buuren MM, Andersen RS, et al. Neoantigen landscape dynamics during human melanoma-T cell interactions. Nature 2016;536:91–5.
24. Curran MA, Montalvo W, Yagita H, Allison JP. PD-1 and CTLA-4 combination blockade expands infiltrating T cells and reduces regulatory T and myeloid cells within B16 melanoma tumors. Proc Natl Acad Sci U S A 2010;107:4275–80.
25. Spranger S, Koblish HK, Horton B, Scherle PA, Newton R, Gajewski TF. Mechanism of tumor rejection with doublets of CTLA-4, PD-1/PD-L1, or IDO blockade involves restored IL-2 production and proliferation of CD8(+) T cells directly within the tumor microenvironment. J Immunother Cancer 2014;2:3.
26. Broz ML, Binnewies M, Boldajipour B, Nelson AE, Pollack JL, Erle DJ, et al. Dissecting the tumor myeloid compartment reveals rare activating antigen-presenting cells critical for T cell immunity. Cancer Cell 2014;26:638–52.
27. Ruffell B, Chang-Strachan D, Chan V, Rosenbusch A, Ho CM, Pryer N, et al. Macrophage IL-10 blocks CD8+ T cell-dependent responses to chemotherapy by suppressing IL-12 expression in intratumoral dendritic cells. Cancer Cell 2014;26:623–37.
28. Wylie B, Seppanen E, Xiao K, Zemek R, Zanker D, Prato S, et al. Cross-presentation of cutaneous melanoma antigen by migratory XCR1+CD103- and XCR1+CD103+ dendritic cells. Oncoimmunology 2015;4:e1019198.
29. Salmon H, Idoyaga J, Rahman A, Leboeuf M, Remark R, Jordan S, et al. Expansion and activation of CD103(+) dendritic cell progenitors at the tumor site enhances tumor responses to therapeutic PD-L1 and BRAF inhibition. Immunity 2016;44:924–38.
30. Roberts EW, Broz ML, Binnewies M, Headley MB, Nelson AE, Wolf DM, et al. Critical role for CD103(+)/CD141(+) dendritic cells bearing CCR7 for tumor antigen trafficking and priming of t cell immunity in melanoma. Cancer Cell 2016;30:324–36.
31. Beavis PA, Milenkovski N, Henderson MA, John LB, Allard B, Loi S, et al. Adenosine receptor 2A blockade increases the efficacy of anti-PD-1 through enhanced antitumor T-cell responses. Cancer Immunol Res 2015;3:506–17.
32. Gilfillan S, Chan CJ, Cella M, Haynes NM, Rapaport AS, Boles KS, et al. DNAM-1 promotes activation of cytotoxic lymphocytes by nonprofessional antigen-presenting cells and tumors. J Exp Med 2008;205:2965–73.
33. Stewart TJ, Abrams SI. Altered immune function during long-term host-tumor interactions can be modulated to retard autochthonous neoplastic growth. J Immunol 2007;179:2851–9.
34. Gubin MM, Zhang X, Schuster H, Caron E, Ward JP, Noguchi T, et al. Checkpoint blockade cancer immunotherapy targets tumour-specific mutant antigens. Nature 2014;515:577–81.
35. Prato S, Zhan Y, Mintern JD, Villadangos JA. Rapid deletion and inactivation of CTLs upon recognition of a number of target cells over a critical threshold. J Immunol 2013;191:3534–44.
36. Engelhardt JJ, Boldajipour B, Beemiller P, Pandurangi P, Sorensen C, Werb Z, et al. Marginating dendritic cells of the tumor microenvironment cross-present tumor antigens and stably engage tumor-specific T cells. Cancer Cell 2012;21:402–17.
37. Oghumu S, Varikuti S, Terrazas C, Kotov D, Nasser MW, Powell CA, et al. CXCR3 deficiency enhances tumor progression by promoting macrophage M2 polarization in a murine breast cancer model. Immunology 2014;143:109–19.
38. Murray PJ, Wynn TA. Protective and pathogenic functions of macrophage subsets. Nat Rev Immunol 2011;11:723–37.
39. Peggs KS, Quezada SA, Chambers CA, Korman AJ, Allison JP. Blockade of CTLA-4 on both effector and regulatory T cell compartments contributes to the antitumor activity of anti-CTLA-4 antibodies. J Exp Med 2009;206:1717–25.
40. Duraiswamy J, Kaluza KM, Freeman GJ, Coukos G. Dual blockade of PD-1 and CTLA-4 combined with tumor vaccine effectively restores T-cell rejection function in tumors. Cancer Res 2013;73:3591–603.
41. Koyama S, Akbay EA, Li YY, Herter-Sprie GS, Buczkowski KA, Richards WG, et al. Adaptive resistance to therapeutic PD-1 blockade is associated with upregulation of alternative immune checkpoints. Nat Commun 2016;7:10501.
42. Ribas A, Shin DS, Zaretsky J, Frederiksen J, Cornish A, Avramis E, et al. PD-1 blockade expands intratumoral memory T cells. Cancer Immunol Res 2016;4:194–203.
43. Ng Tang D, Shen Y, Sun J, Wen S, Wolchok JD, Yuan J, et al. Increased frequency of ICOS+ CD4 T cells as a pharmacodynamic biomarker for anti-CTLA-4 therapy. Cancer Immunol Res 2013;1:229–34.
44. Kool M, Soullie T, van Nimwegen M, Willart MA, Muskens F, Jung S, et al. Alum adjuvant boosts adaptive immunity by inducing uric acid and activating inflammatory dendritic cells. J Exp Med 2008;205:869–82.
45. Sheng J, Chen Q, Soncin I, Ng SL, Karjalainen K, Ruedl C. A discrete subset of monocyte-derived cells among typical conventional type 2 dendritic cells can efficiently cross-present. Cell Rep 2017;21:1203–14.
46. Movahedi K, Laoui D, Gysemans C, Baeten M, Stange G, Van den Bossche J, et al. Different tumor microenvironments contain functionally distinct subsets of macrophages derived from Ly6C(high) monocytes. Cancer Res 2010;70:5728–39.
47. Hildner K, Edelson BT, Purtha WE, Diamond M, Matsushita H, Kohyama M, et al. Batf3 deficiency reveals a critical role for CD8alpha+ dendritic cells in cytotoxic T cell immunity. Science 2008;322:1097–100.
48. de Mingo Pulido A, Gardner A, Hiebler S, Soliman H, Rugo HS, Krummel MF, et al. TIM-3 regulates CD103(+) dendritic cell function and response to chemotherapy in breast cancer. Cancer Cell 2018;33:60–74.
49. Mittal D, Vijayan D, Putz EM, Aguilera AR, Markey KA, Straube J, et al. Interleukin-12 from CD103(+) Batf3-dependent dendritic cells required for NK-cell suppression of metastasis. Cancer Immunol Res 2017;5:1098–108.

50. Yin P, Liu X, Mansfield AS, Harrington SM, Li Y, Yan Y, et al. CpG-induced antitumor immunity requires IL-12 in expansion of effector cells and down-regulation of PD-1. Oncotarget 2016;7:70223–31.
51. Ngiow SF, Young A, Blake SJ, Hill GR, Yagita H, Teng MW, et al. Agonistic CD40 mAb-driven IL12 reverses resistance to anti-PD1 in a T-cell-rich tumor. Cancer Res 2016;76:6266–77.
52. Bennett SR, Carbone FR, Karamalis F, Miller JF, Heath WR. Induction of a CD8+ cytotoxic T lymphocyte response by cross-priming requires cognate CD4+ T cell help. J Exp Med 1997;186:65–70.
53. Hor JL, Whitney PG, Zaid A, Brooks AG, Heath WR, Mueller SN. Spatiotemporally distinct interactions with dendritic cell subsets facilitates CD4+ and CD8+ T cell activation to localized viral infection. Immunity 2015;43:554–65.
54. Eickhoff S, Brewitz A, Gerner MY, Klauschen F, Komander K, Hemmi H, et al. Robust anti-viral immunity requires multiple distinct T cell-dendritic cell interactions. Cell 2015;162:1322–37.
55. Wei SC, Levine JH, Cogdill AP, Zhao Y, Anang NAS, Andrews MC, et al. Distinct cellular mechanisms underlie anti-CTLA-4 and anti-PD-1 checkpoint blockade. Cell 2017;170:1120–33e17.